Proceedings of ASME Turbo Expo 2013: Turbine Technical Conference and Exposition
GT2013
June 3-7, 2013, San Antonio, Texas, USA

GT2013-96005

CREEP CRACK GROWTH SIMULATION OF NI-BASE SUPERALLOY

Calvin M. Stewart
Department of Mechanical, Materials, & Aerospace Engineering, University of Central Florida
Orlando, FL USA 32816-2450

Ali P. Gordon
Department of Mechanical, Materials, & Aerospace Engineering, University of Central Florida
Orlando, FL USA 32816-2450

ABSTRACT

The purpose of this study is to develop a numerical approach to simulate the creep cracking of a Ni-base superalloy. The approach is based in continuum damage mechanics (CDM) and uses the classic Kachanov-Rabotnov constitutive equations for creep deformation and damage evolution. Creep damage takes the form of defects such as microcracks, cavities, voids, etc. A numerical crack growth algorithm is developed to predict the onset of crack initiation and the successive growth of cracks via element death in the general purpose finite element software ANSYS. In this paper, the Kachanov-Rabotnov constitutive model is implemented as a user material model in ANSYS and the numerical crack growth algorithm is developed and written in ANSYS parametric design language (APDL) command code. A study of mesh size in relation to initial flaw size and initiation time is performed. A demonstration of the proposed numerical crack growth algorithm is performed and a qualitative analysis conducted. A series of improvements and parametric studies are suggested for future work.

KEYWORDS: Creep Deformation, Continuum Damage Mechanics (CDM), Kachanov-Rabotnov, Numerical Crack Growth, Crack Initiation

1. INTRODUCTION

In the nuclear power industry, the fundamental damage mechanisms are creep, fatigue (mechanical, fretting, and/or thermal fatigue), creep-fatigue interaction (isothermal-CF or thermomechanical fatigue-TMF), corrosion, and irradiation. High cycle thermal fatigue is observed in pressured water reactor (PWR) piping [1]. Neutron absorber rods are susceptible to creep crack growth and irradiation damage [2]. Fretting is observed in nuclear fuel rods, steam generator tubes and control roads [3].

A significant effort has gone towards understanding the problem of creep damage and crack growth. For metals at temperatures above 30% of melting temperature and under sustained mechanical load, over time microstructural defects can coalesce to form a crack. The crack may propagate until fracture of a member. The nucleation of multiple cracks within a single member has a high probability when the member is under complex load. The management of surface and subsurface cracks has inspired a myriad of experimental non-destructive techniques (NDT) that are used in service to manage remaining life [4]. An alternative approach is to (during the design phase) develop an appropriate model to predict crack initiation and propagation and implement that model within a finite element environment. This technique could be used to optimize geometry and boundary conditions such that creep cracks arrest.

A number of linear elastic fracture mechanics (LFEM) based computer codes exist to model crack growth (FRANC2D, FRANC3D, FEACrack, CurvedCrack, ADAPCrack3D, ZenCrack, BEASY, XFEM) [5]. A majority of these codes are third-party extensions to established FEM software; requiring that the crack propagation information be calculated externally after each iteration. The mesh and/or geometry are modified and an updated FE model provided to the solver (ANSYS, ABAQUS, and Nastran). This process is repeated iteratively until some fracture criterion is reached. The crack direction is based on one of the following criteria: Griffith's maximum energy release rate (the direction where the energy release rate is maximum) [6], maximum circumferential stress criterion (normal to the direction of the maximum hoop stress) [7], minimum strain energy density criterion (normal to the direction of minimum strain energy) [8], or minimum mode II stress intensity factor (along the direction where mode II SIF vanishes) [9]. The crack increment Δa is typically provided based on some variation

of the Paris law. In many cases, the Paris law is too simplistic to accurately predict crack growth in practical problems.

Damage in metals is a process of initiation and propagation of defects through a member. Damage is an irreversible heterogeneous process dependent on boundary conditions, metallurgical history, time and environment. At the atomic-scale the state of damage is based on edge, screw, and mixed dislocations. At the micro-scale damage is determined by the number, size, and configuration of micro-cracks and micro-voids [10]. At the macro-scale damage is determined by the grain boundary sliding and macro-void and crack coalesce. The macro-scale is the scale of the representative volume element (RVE). The RVE is regarded as the smallest volume statistically representative of the mean constitutive response and that includes a representative number of micro-heterogeneities. The continuum concept involves transferring from the physical space of the heterogeneously damaged RVE (ε, σ), to an effective space of a homogenous undamaged RVE using effective state variables $(\tilde{\varepsilon}, \tilde{\sigma}, \omega, R, D)$ where ω represents damage density and *R* and *D* are isotropic and kinematic hardening variables respectively [11]. This approach can be quickly implemented into the finite element method by equating a finite element to a RVE. The continuum damage mechanics (CDM) approach has been used to model elastic-brittle, elastic-plastic, spall, fatigue, creep, creep-fatigue (isothermal and thermomechanical), anisotropic, corrosion, and irradiation driven damage.

LEFM has a number of limitations when compared to CDM when simulating crack growth [12]. It either requires a new geometry and mesh at each step during propagation or local enrichment of approximation space through the partition of unity concept (PUFEM) (meshless). Plasticity at the crack tip requires a plastic zone correction that is only valid at moderate plastic strain. The stress intensity factor is dependent on specimen geometry and loading conditions. The study of crack initiation and propagation are typically modeled using different parameters. The effect of load history is often ignored. Alternatively, CDM can predict behavior before crack initiation, be quickly implemented into FEM, and readily applied to component shaped geometry.

A successful CDM-based numerical crack growth simulation technique requires the following:

- A mesh with RVEs of appropriate size along the probable crack path.
- A constitutive model to establish the stress-strain field in the member and about the crack tip
- A CDM-based damage law to establish the damage state of the RVEs
- A numerical crack growth algorithm to identify the rupture of RVEs, direction of crack growth, disables ruptured RVEs, and automatically computes an approximate time step where the next RVE will fail.

In the following paper, the Kachanov-Rabotnov creep-damage constitutive model will be used to determine the damage state variable and define the stress-strain field. A numerical crack growth algorithm will be written in APDL command code to propagate the crack using the commercial ANSYS FEA software. An input deck written in APDL command code will be used to generate geometry, apply boundary conditions, call constitutive models, and set material properties. A series of simulations will be conducted to evaluate the influence mesh size has on crack initiation time. Preliminary results for crack propagation will be reported. Finally, conclusions are formed and future work suggested.

2. CONSTITUTIVE MODEL

Creep deformation is defined in three distinct stages: primary, secondary, and tertiary. During the primary creep regime, dislocations slip and climb. Eventually a saturation of dislocation density coupled with recovery mechanics in balance form the secondary creep regime. Finally, the tertiary creep regime is observed where grain boundaries slide, voids form and coalesce leading to rupture. The tertiary creep regime is where damage evolves.

To account for the tertiary creep damage behavior of materials, Kachanov [13] and Rabotnov [14] developed the first Continuum Damage Mechanics (CDM) based isotropic creep-damage formulation. Damage is an all inclusive, non-recoverable accumulation that exhibits the same dependencies as creep deformation: material behavior (i.e., creep constants), temperature, time, and stress. The Kachanov-Rabotnov equations for the creep rate and damage evolution are as follows

$$\dot{\varepsilon}_{cr} = \frac{d\varepsilon_{cr}}{dt} = A\left(\frac{\bar{\sigma}}{1-\omega}\right)^{n} \tag{1}$$

$$\dot{\omega} = \frac{d\omega}{dt} = \frac{M\bar{\sigma}^{\chi}}{(1-\omega)^{\phi}} \tag{2}$$

where the creep strain rate is equal to Norton's power law for secondary creep with the same associated *A* and *n* constants, $\bar{\sigma}$ is von Mises stress, and *M*, χ, and ϕ are tertiary creep damage constants [15]. The secondary and tertiary creep damage constants can be determined using an appropriate analytical technique [16]. An isochoric creep behavior (incompressibility) is assumed. Rupture predictions can be easily arrived at using damage evolution, Eq. (2). Separation of variables, integration, and simplification furnishes the following

$$t_r - t_0 = \frac{(1-\omega_0)^{\phi+1} - (1-\omega_{cr})^{\phi+1}}{(\phi+1)M\bar{\sigma}^{\chi}} \tag{3}$$

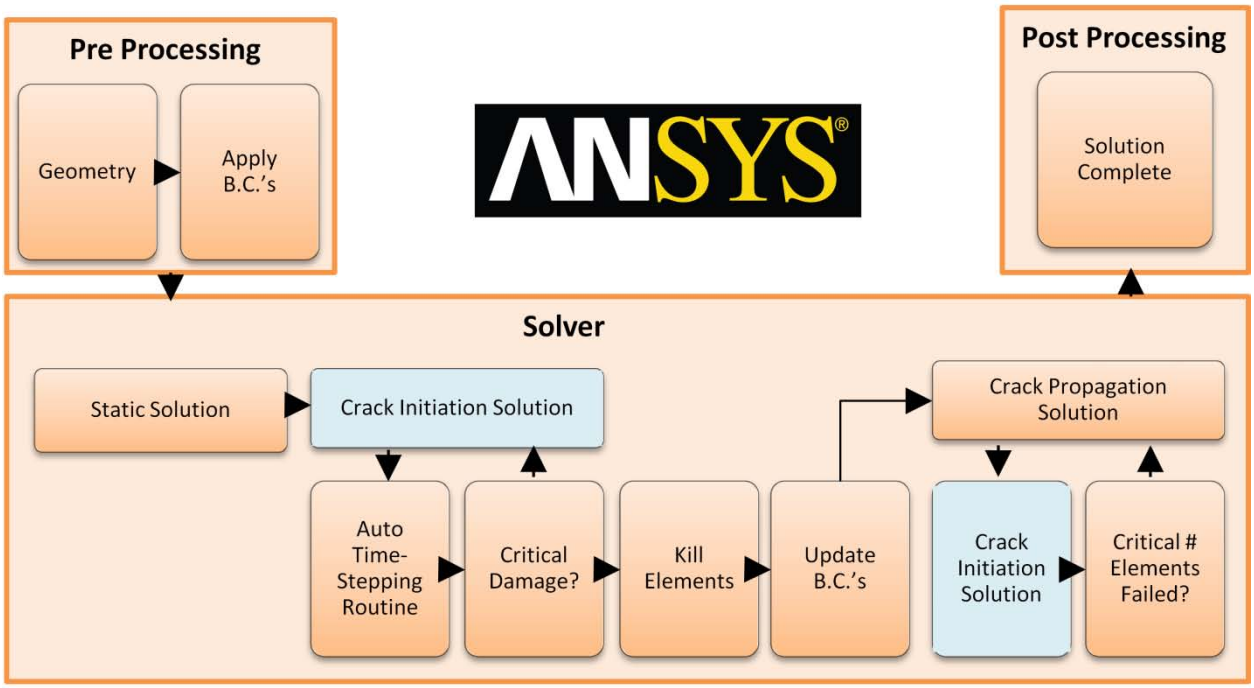

Figure 1 - Flow chart of numerical crack growth algorithm

where t_r is the rupture time, ω_{cr} is critical damage, and t_0 and ω_0 are the initial time and damage respectively. Typically, ω_{cr} is assumed to be unity. Numerous authors have developed specialized variations based on this fundamental formulation [17-20].

The commercial finite element software ANSYS is used in this study. ANSYS contains a parametric design language (APDL), a scripting language that allows users to access all ANSYS commands and build a model in terms of parameters. ANSYS has an open architecture which allows users to write routines and/or subroutines in C or FORTRAN and link them to ANSYS as user-programmable features (UPF). A FORTRAN USERCREEP.F code is written to model the Kachanov-Rabotnov creep deformation and the coupled creep-fatigue damage law.

3. NUMERICAL CRACK GROWTH ALOGRITHM

For the best of two to three decades, research has been conducted on numerical crack propagation modeling [21-23]. A number of finite element methods (FEM) can be used: classical (FEM), partition of unity (PUFEM), generalized (GFEM), smoothed (SFEM), node-based smoothed (NS-FEM), edge-based smooth (ES-FEM), and extended (XFEM) [21]. The earliest and most common is classic FEM where crack propagation is modeled using element removal and/or adaptive remeshing algorithms. In work by Bogard et al., fatigue crack propagation is simulated using a user-developed element removal and adaptive remeshing algorithm within commercial ABAQUS software [22]. Crack propagation is approximated by a CDM-based stress amplitude damage law. In Gyllenskog's thesis, fatigue crack propagation is simulated using an element removal algorithm within commercial ANSYS software [23]. Crack propagation is approximated using the Basquin stress-life equation and the Palmgren-Miner damage law.

In this study, the numerical crack growth algorithm is developed using ANSYS APDL. The advanced analysis feature called "Element Birth & Death" is used to remove elements that fail during a simulation. This feature effectively removes elements by reducing the selected elements stiffness by a factor of 1E-16. The numerical crack growth algorithm can be divided into three stages: pre-processing, solver and post processing. A flow chart of the numerical crack growth algorithm is provided in Figure 1. During the pre-processing stage the element type, geometry, and boundary conditions are defined. During the solver stage the static, crack initiation, and crack growth solutions are solved. The static solution is used to establish the elastic stress-strain field within the geometry. The crack initiation solution calls the Kachanov-Rabotnov creep-damage constitutive model and the crack initiation algorithm. In the crack initiation algorithm a custom automatic time-stepping routine is used to converge towards a solution where the first element has failed and is removed. When the first element has failed it can be assumed that a crack has initiated where the flaw size is equal to the mesh size (element edge length). The crack propagation solution calls the crack propagation algorithm. This algorithm iteratively uses the crack initiation algorithm to simulate the crack growth process. The direction of crack growth is defined as follows: The crack must grow in an element (adjacent to the crack front) that has reached critical damage at an angle between 90 and 270° perpendicular to the previous crack direction. This is

Table 1 - Nominal Chemical Composition of Hastelloy X (wt%)

Cr	Fe	Mo	Mn	Co	W	Si	Al
21.91	19	8.65	0.82	0.79	0.44	0.42	0.17
Cu	**C**	**N**	**P**	**Ti**	**B**	**S**	**Ni**
0.13	0.082	0.015	0.013	0.007	0.002	0.0003	Bal

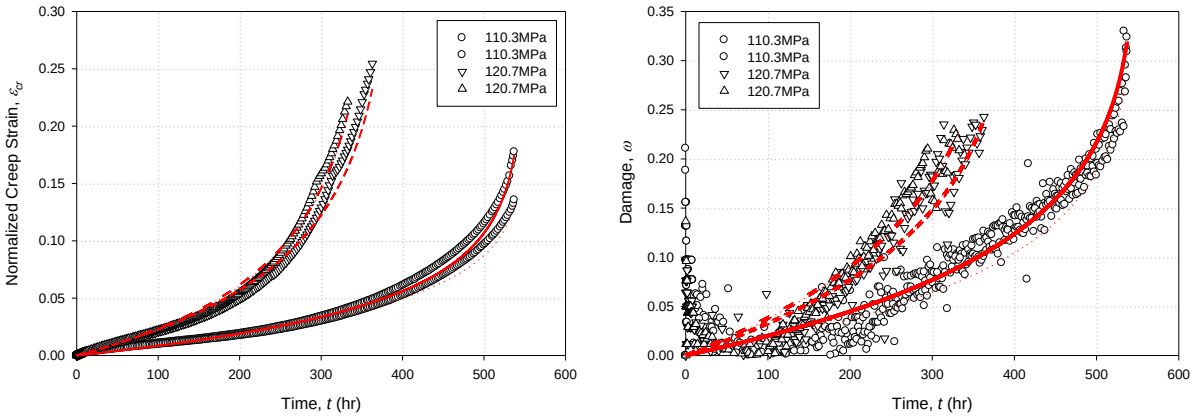

Figure 2 - Creep deformation and damage evolution of Hastelloy X at 760°C

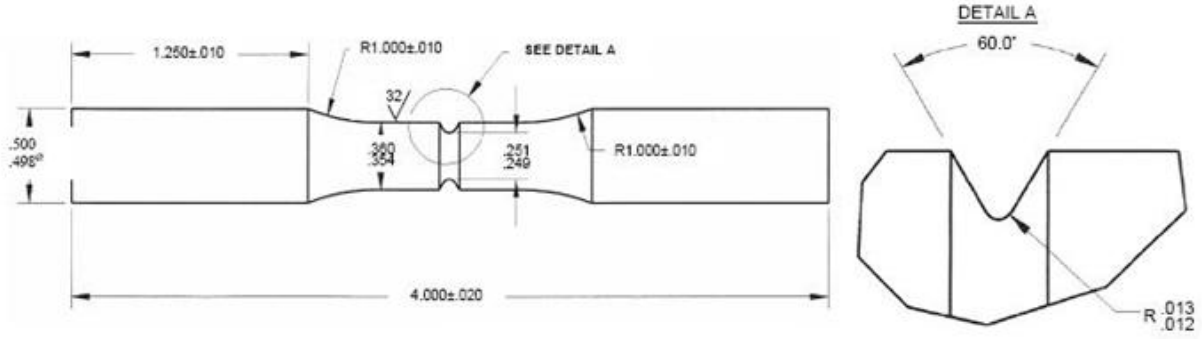

Figure 3 - Notched specimen geometry (units in inches)

geometrically achieved by preventing crack growth in elements attached to the dead element behind the current crack front (this geometric approach has not been validated for degenerate triangular elements). The iterations continue until a user-defined number of elements have failed or rupture has been encountered and the solution interrupted. The crack is propagated one element at a time which improves accuracy by allowing stress redistribution to occur at the RVE level near the crack tip. Once, rupture has occurred the post-processing stage is entered. During the post-processing stage the deformation, damage, and crack properties are analyzed. FE results are stored at every time increment. A contour plot of damage is created at each step where an element has been removed.

The custom automatic time-stepping routine can be described as follows. A time-step factor is calculated in the USERCREEP.F UPF at every increment. This time-step factor is the rupture time prediction [Eq. (3)] inverted and modified for iteration as follows

$$\frac{1}{\Delta t}=\frac{1}{t_{i+1}-t_i}=\frac{(\phi+1)M\bar{\sigma}^{\chi}}{(1-\omega_i)^{\phi+1}-(1-\omega_r)^{\phi+1}} \tag{4}$$

where ω_{cr} is critical damage, t_{i+1} is the predicted rupture time, and t_i and ω_i are the current time and damage respectively. This inverted form is necessary to prevent the numerical singularity observed in elements that have infinite life. When $\omega_i \square \omega_{cr}$ then $1/\Delta t$ is set to zero to prevent the time-step from reducing to an infinitely small number. Once the current time-step is solved, the nodal solution of the time-step factor is plotted and the maximum value located and made a parameter. This parameter is inverted and gives the next time-step increment. The usefulness of this approach is that the time-step increment is based on the time needed for the next element to fail.

If stress was held constant and no relaxation was to occur, the exact time increment needed for crack initiation would be determined by the time-step factor [Eq. (4)]; however, in real life (and the FE model) stress relaxation and redistribution occurs at the crack tip due to creep deformation and crack tip

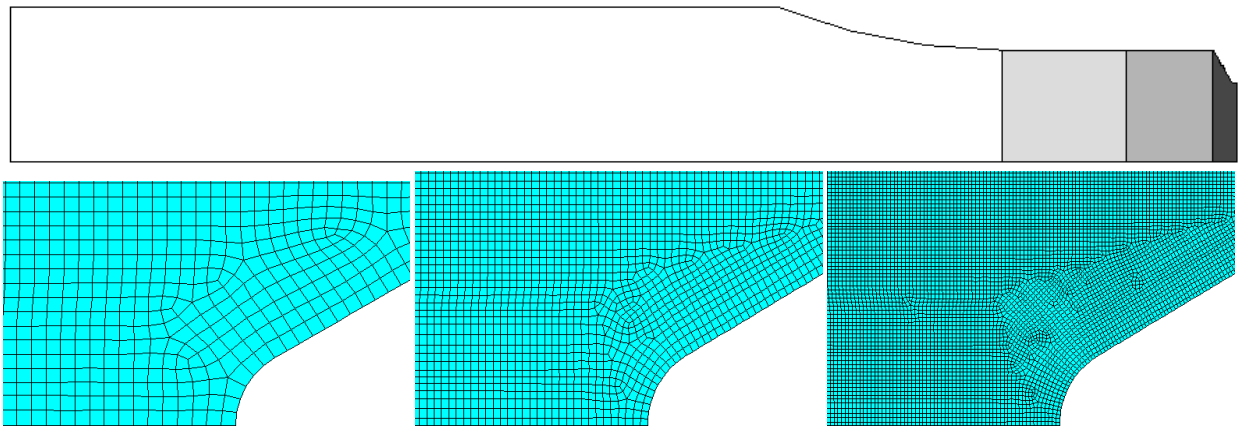

Figure 4 - Mesh at the notch for three different element edge lengths

Table 2 - Mesh Sensitivity of V-notch specimen model in ANSYS

Mesh	Mesh Size (element edge length, mm)				Number of		Elastic SCF, K_t	CPU Time
	Notch	Near Notch	Reduced	Grip	Elements	Nodes		*s*
1	0.06	0.25	0.5	1	3203	9850	7.57	3.292
2	0.03	0.25	0.5	1	8086	24595	7.62	8.923
3	0.015	0.25	0.4	1	23907	72238	7.63	25.132

movement. The sub-steps size (multiple sub-steps are taken within each calculated time increment) influences the creep deformation and damage evolution; thus the automatic time-stepping routine under predicts the next time increment. This issue is overcome numerically when the current damage reaches critical, $\omega \geq \omega_{cr}$. The number of iterations needed to solve a solution is directly related to the complexity of geometry and boundary conditions. Complex structures increase the number of iterations needed to solve a particular solution.

4. PRELIMINARY RESULTS

The subject material is wrought Hastelloy X (HX), a Ni-Cr-Fe solid-solution-strengthened Ni-base superalloy. The nominal chemical composition is provided in Table 1. The microstructure of HX consists most of equiaxial face-centered-cubic (FCC) 95µm grains with some annealing twins. The material exhibits great strength, oxidation and corrosion resistance at temperatures up to 1093°C (2000°F). Due to these properties it has been used extensively in the power generation industry. A large number of studies have been performed on this material characterizing the tensile, rupture, and creep deformation behavior [24-27].

A set of constant-load tensile creep tests were performed at a load of 110.3MPa and 120.7MPa and temperature of 760°C following ASTM Standard [28]. The secondary creep and tertiary creep damage constants *A*, *n*, *M*, χ, and ϕ where determined analytically using a procedure previously developed by the authors [16]. The secondary creep constants *A* and *n* were found to be 1.6110E-25 $MPa^{-n}hr^{-1}$ and 10.269 respectively. The tertiary creep constants *M*, χ, and ϕ were averaged to 15.19E-11 $MPa^{-\chi}hr^{-1}$, 3, and 8.567 respectively. Figure 2 shows the fit of the analytical constants to the creep deformation and damage evolution respectively where the lines represent simulations and points represent experimental data.

The V-notched geometry was adopted from previous research and is shown in Figure 3 [29]. The notched geometry follows the ASTM Standard Test method for Sharp-Notch Tension Testing with Cylindrical Specimens [30]. The V-notched geometry is replicated as a 2D model with 8-noded PLANE183 elements.

In FEM the geometry is separated into notch, near notch, reduced, and grip areas. Each area is given a different mesh size with the smallest applied to the notch. A series of static elastic simulations in tension are conducted to evaluate mesh sizing. Three mesh sizes were evaluated and are depicted in Figure 4. Mesh sensitivity is characterized by the value of the elastic stress concentration factor (SCF), *K*. A table of the mesh size, number of nodes and elements, and the resulting *K* is provided in Table 2. The elastic SCF increased slightly as mesh size is decreased. A metric for the accuracy of a solution is the error between the nodal and element solution. The nodal solution is the averaged solution while the element solution is un-averaged. In all cases the element and nodal solution were equal demonstrating that the stress field calculated in the element from the shape functions is continuous. All three meshes are of appropriate size.

In the static solution, when the nodal and element solutions are equal the error between FEM and experimental SCF will be minimal. Under time-dependent creep crack initiation and propagation it is possible that mesh size can influence stress-relaxation and redistribution causing computational errors.

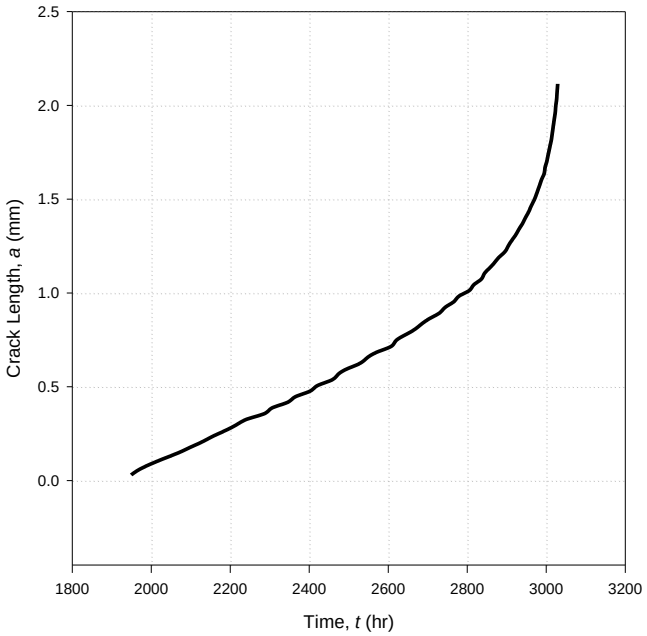

Figure 5 - Crack length versus time

Table 3 - Crack Initiation Results of Hastelloy X at 30MPa and 760°C

Time	Mesh Size	CPU Time	Length of Initial Flaw
hr	*mm*	*s*	*mm*
2011.042	*0.06*	*178*	*5.90E-02*
2948.6	*0.03*	*381*	*2.98E-02*
1959.881	*0.015*	*1215*	*2.99E-02*

To that end, a study on the creep crack initiation behavior of the three meshes was conducted. Simulations were conducted at 30 MPa and 760°C. The low stress was applied due to the stress concentration found at the notch tip. Critical damage ω_{cr} was set to 0.33 the maximum observed in Figure 2. The time increment was calculated using the automatic time-stepping algorithm. The minimum and maximum sub-step size was set to 10^{-3} and 50 hours respectively. The creep criterion that controls automatic sub-step time increment (built into ANSYS) was set to 10. The results of the study are provided in Table 3. It is observed that the length of initial flaw and crack initiation time have a linear relationship with an R^2 value of 0.9722. (The small error is incurred due to the maximum sub-step size, to be discussed later) This shows that once nodal and element solutions are equal; mesh size does not influence crack initiation. Crack initiation time depends on the initial flaw size assumed. The a priori assumed initial flaw size should be set as the mesh size at the stress concentration and along the probable crack path. It is observed that the CPU time and mesh size have a power-law decay relationship with an R^2 value of .9858. As mesh size is reduced the CPU time necessary to complete the solution increases by a power. This demonstrates that the mesh size and subsequently assumed initial flaw size should be chosen carefully to avoid long solution completion time. While the automatic time-stepping routine was designed to calculate the appropriate time-step needed to fail only a single element; in some cases more than one element can fail. This was observed in the 0.015 mesh solution. This issue occurs when the maximum sub-step increment is too large. The size of the sub-step increment directly influences the stress-strain and damage evolution due to the rate-dependent response of the constitutive model. Sub-step size must be optimized to prevent multi-element failure while also maintaining CPU time efficiency. Future work should include a parametric investigation of the influence sub-step size, notch geometry and element shape have on crack initiation.

The crack propagation solution is still in the prototype stage. The memory usage and results file storage have not been formally optimized resulting in long CPU time (>24hours) for completion of a solution. To that end, only a simulation of the 0.03 mm mesh size was conducted. A qualitative analysis of the results follows. The crack is observed to propagate perpendicular to the applied load. This would be observed in an experiment conducted on the v-notched specimen under tension. A plot of crack length versus time is provided in Figure 5. It is observed that an exponential rise relationship exists between crack length and time. This behavior is similar to that observed in notched specimen of various metals. Contour plots of the damage field at various stages of crack growth are provided in Figure 6. It is observed that initially a high gradient damage field is observed at the crack tip. Over time the field disperses across the geometry. The damage field near the crack tip is observed to expand as the length of the crack increases. The crack maintains a linear path. This can be attributed to crack direction constraint built into the crack propagation algorithm. The stress field is observed to lead the crack initially. At intermediate crack length, a low stress begins to develop behind the crack tip. At long crack length the stress behind the crack tip becomes the maximum in the body. Further analysis of this behavior must be conducted. An instant fracture criterion has not been built into the command code; therefore, it is not known at what time the results should be neglected and failure assumed. The strain field is observed to lead the crack always. At long crack lengths the maximum strain observed increases dramatically.

With proper constant optimization to experimental data the numerical crack growth technique can be used to predict crack propagation rates.

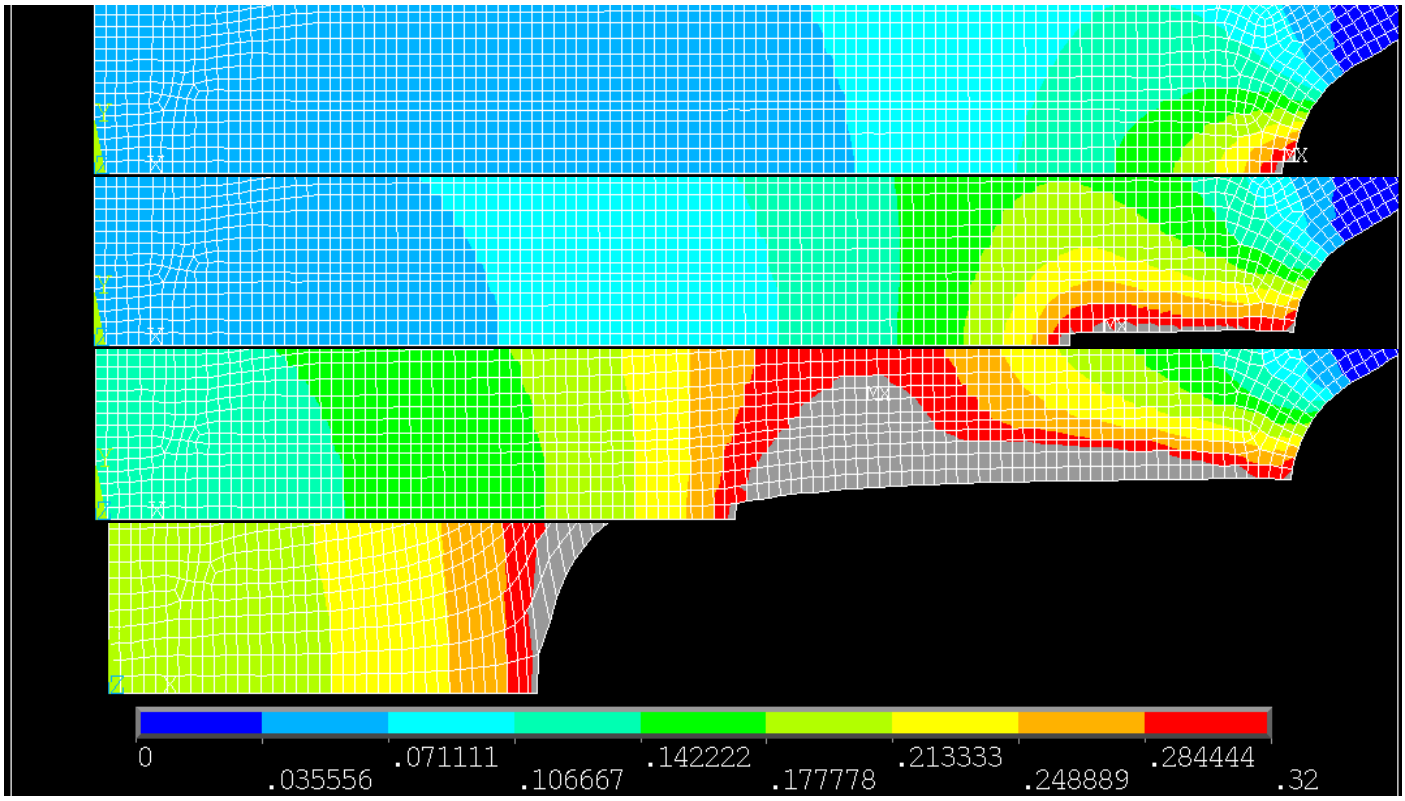

Figure 6 - Contour Plots of Damage at 1, 20, 50 and 70 failed elements

5. CONCLUSION

It is demonstrated that crack initiation and propagation can be simulated using a numerical crack growth algorithm in the ANSYS finite element software. The empirical relationship of flaw size versus initiation time and crack length versus time duplicates that observed in literature. It is hypothesized that using only smooth constant-load tensile specimen data the behavior of notched specimen before and during crack initiation and propagation can be predicted using the numerical crack growth technique. The following future work will be conducted to evaluate this hypothesis:

- A parametric investigation of the influence notch geometry has on crack initiation and propagation.
- An investigation into crack initiation and propagation using degenerate triangular elements
- An investigation into crack behavior on a non-symmetric geometry
- A study on the relationship between mesh size and propagation rates.
- The addition of instant fracture criterion
- Optimization of the APDL command code. The elimination of superfluous commands to speed up CPU time. Improved calculation of sub-step size using the built in ANSYS routine (via the creep criterion). Improved calculation of time increment using the automatic time-stepping routine. Improved memory usage. Minimization of the results file.
- A comparison of notched experimental data with that obtained from numerical crack growth simulations using constants characterized from smooth constant-load tensile specimen.

6. ACKNOWLEDGEMENTS

Calvin Stewart is thankful for the support of a McKnight Doctoral Fellowship through the Florida Education Fund. Ali P. Gordon recognizes the support of the Florida Center for Advanced Aero-Propulsion (FCAAP).

REFERENCES

[1] Simos, N., Reich, M., Hartzman, M., and Costantino, C. J., 1990, "Assessment of Thermal Fatigue Crack Propagation in Safety Injection PWR Lines," Pressure vessels and piping conference: be in tune for the 90's, Nashville, TN (USA), 17-21 Jun 1990.

[2] Yokoyama, N., Tsuji, H., Tsukada, T., and Shindo, M., 1997, "Development of Comprehensive Material Performance Database for Nuclear Applications," *Computerization and Networking of Material Databases*, **5**, pp. 261-272.

[3] Lee, Y. H., and Kim, H. K., 2007, "Development of a Fretting Wear Evaluation Method in the Nuclear Fuel Fretting by using a Wear Scar Shape," *Advanced Materials Research*, **26-28**, pp. 1231-1234.

[4] Saburov, Y., Kazys, R., and Sliteris, R., 2001, "NDT Activity in the Ignalina Nuclear Power Plant," *Insight-Non-Destructive Testing and Condition Monitoring*, **43**(6), pp. 372-375.
[5] Fortino, S., And Bilotta, A., 2004, "Evaluation of the Amount of Crack Growth in 2D LEFM problems," *Engineering Fracture Mechanics*, **71**(9-10), pp. 1403-1419.
[6] Nuismer, R. J., 1975, An Energy Release Rate Criterion for Mixed Mode Fracture, *International Journal of Fracture*, **11**, pp. 245-250.
[7] Erdogan, F., and Sih G., 1963, "On the Crack Extension in Plates under Plane Loading and Transverse Shear," *Journal of Basic Engineering*, **85**, pp.519-527.
[8] Sih, G., 1974, "Strain Energy Density Factor applied to Mixed Mode Crack Problems," *International Journal of Fracture*, **10**, pp. 305-321.
[9] Goldstein, R V and Salganik, R L, 1974, "Brittle Fracture of Solids with Arbitrary Cracks", *International Journal of Fracture*, **10**(4),pp. 507-523.
[10] Voyiadjis, G. Z., and Kattan, P. I., 2005, *Damage Mechanics*, CRC Press, Boca Raton, FL.
[11] Skrzypek, J. and Ganczarski, A., 1999, *Modeling of Material Damage and Failure of Structures: Theory and Applications*, Springer, Berlin, Germany.
[12] McDowell, D., 1997, *Application of Continuum Damage Mechanics to Fatigue and Fracture*, American Society for Testing and Materials, West Conshohocken, PA.
[13] Kachanov, L. M., 1967, *The Theory of Creep*, National Lending Library for Science and Technology, Boston Spa, England, Chaps. IX, X.
[14] Rabotnov, Y. N., 1969, *Creep Problems in Structural Members*, North Holland, Amsterdam.
[15] Norton, F. H., 1929, *The creep of steel at high temperatures*, McGraw-Hill, London.
[16] Stewart, C. M., and Gordon A. P., 2011, "Strain and Damage-Based Analytical Methods to Determine the Kachanov-Rabotnov Tertiary Creep Damage Constants," *International Journal of Damage Mechanics*, Dec 21st, 2011.
[17] Stewart C. M., and Gordon A. P., (2009), "Modeling the Temperature Dependence of Tertiary Creep Damage of a Ni-base Alloy," *Journal of Pressure Vessel Technology*, **131**(5), pp.1-11.
[18] Stewart C. M., Gordon A. P., Ma, Y. W., and Neu, R. W., 2011, "An Improved Anisotropic Tertiary Creep Damage Formulation," *Journal of Pressure Vessel Technology*, **133**(5), pp. 1-10.
[19] Stewart C. M., Gordon A. P., Ma, Y. W., and Neu, R. W., (2011), "An Anisotropic Tertiary Creep-Damage Constitutive Model for Anisotropic Materials," *International Journal of Pressure Vessel and Piping*, **88**(8-9), pp. 356-364.
[20] Stewart, C. M., and Gordon A. P., (2012), "Constitutive Modeling of Multistage Creep Damage in Isotropic and Transversely-Isotropic Alloys with Elastic Damage," *Journal of Pressure Vessel Technology*, Accepted For Publication.
[21] Nourbakhshnia, N., and Liu, G. R., 2011, "A Quasi-Static Crack Growth Simulation Based on the Singular ES-FEM," *International Journal for Numerical Methods in Engineering*, **88**(5), pp. 473-492.
[22] Bogard, F., Lestriez, P., and Guo, Y. Q., 2010, "Damage and Rupture Simulation for Mechanical Parts Under Cyclic Loadings," *Journal of Engineering Materials and Technology*, **132**(2), pp. 1-8.
[23] Gyllenskog, J. D., 2010, "Fatigue Life Analysis of T-38 Aileron Lever using a Continuum Damage Approach," *Utah State University, M.S. Thesis, Paper 747*, Logan, UT.
[24] Lee, S.Y., et al, 2008, "High-Temperature Tensile-Hold Crack-Growth Behavior of HASTELLOY X alloy compared to HAYNES 188 and HAYNES 230 alloys," *Mechanics of Time-Dependent Materials*, **12**(1), pp. 31-44.
[25] Haynes International, "High Performance Alloys Technical Information: Hastelloy X Alloy," [Online]. Available: http://www.haynesintl.com/pdf/h3009.pdf [Accessed: 6/6/2011]
[26] Kim, W. G., Yin, S. N., Ryu, W. S., and Chang, J. H., 2006, "Creep Properties of Hastelloy-X Alloy for the High Temperature Gas-Cooled Reactor," *Key Engineering Materials*, **326**, pp. 1105-1108.
[27] Kim, W. G., Yin, S. N., Kim, Y.W., and Chang, J. H., 2006, "Creep Characterization of a Ni-based Hastelloy-X Alloy by using Theta Projection Method," *Engineering Fracture Mechanics*, **75**, pp. 4985-4995.
[28] ASTM E-139, "Standard Test Methods for Conducting Creep, Creep-Rupture, and Stress Rupture Tests of Metallic Materials, ASTM E-139 No. 03.01, West Conshohocken, PA.
[29] Kupkovits, R. A., 2008, *Thermomechanical Fatigue Behavior of the Directionally-Solidified Nickel-Base Superalloy CM247LC*, In: *M.S. Thesis*, Georgia Institute of Technology, Atlanta, GA.
[30] ASTM, "ASTM Standard Test Method for Sharp-Notch Tension Testing with Cylindrical Specimens", ASTM E602-03, West Conshohocken, PA.